

EXPERIMENTAL STUDY OF CO-COMBUSTION CHARACTERISTICS AND POLLUTANT EMISSION CHARACTERISTICS OF COAL AND RICE HUSK/ POPULUS TOMENTOSA SAWDUST

Bohan Gu¹, Zhaoping Zhong^{1,}, Qi Xiong¹, Yuxuan Yang^{2,3}, Zekun Yun¹*

^{*1}Key Laboratory of Energy Thermal Conversion and Control of Ministry of Education, School of Energy and Environment, Southeast University, Nanjing 211189, China

²Taizhou Institute of Zhejiang University, Zhejiang University, Taizhou, 318000, China.

³State Key laboratory of Clean Energy Utilization, Institute for Thermal Power Engineering, Zhejiang University, Hangzhou, 310027, China

* Corresponding author; E-mail: zzhong@seu.edu.cn

This investigation examines the co-combustion behavior and pollutant emission patterns of coal blended with two biomass types—rice husk (RH) and Populus tomentosa sawdust (SD)—at varying mixing ratios. Utilizing thermogravimetric analysis (TGA) and a drop-tube furnace system, the combustion performance and emission characteristics were systematically evaluated. The results show that co-firing with RH or SD can effectively improve the combustion performance of coal, and both coupled combustion mechanisms conform to the diffusion model. By comparing the theoretical and experimental values of thermogravimetric curves, it is found that in the main combustion range of 400 °C~570 °C, the interaction between coal and RH/SD first inhibits combustion and then promotes combustion, with the transition occurring around 500 °C. The low sulfur content in RH and SD is the main factor for reducing SO₂ emissions. However, there is a significant difference in their nitrogen content, while their NO_x emission reduction capabilities are not significantly different—with a difference of only 1.89 % when the blending ratio is 25 %. This indicates that co-firing biomass with high nitrogen content can still effectively reduce NO_x emissions. For this reason, a possible NO_x emission reduction mechanism is proposed.

Key words: coal; biomass; co-combustion; pollutant emissions

1 Introduction

As the predominant fossil fuel in China, coal continues to play a central role in the national energy mix. In alignment with the national “dual carbon” strategy, there is an increasing emphasis on transitioning coal-fired power generation toward cleaner and low-carbon operations [1]. Biomass is a renewable and clean energy source. China is rich in biomass resources, with agricultural and forestry wastes as typical representatives [2]. For example, a large amount of waste rice husks are generated during rice production, and a large amount of sawdust is also accompanied during the production and processing processes of *Populus tomentosa*, a fast-growing arbor. However, traditional biomass treatment methods include on-site incineration or discarding, which pose problems of resource waste and environmental pollution. Therefore, co-firing biomass with coal can not only effectively reduce carbon emissions, but also make full use of the advantages of coal-fired units, such as large capacity and high parameters [3]. It is one of the effective approaches to achieve large-scale utilization of biomass resources.

The distinct physicochemical properties of coal and biomass lead to significant alterations in combustion behavior when fired together, moving beyond the characteristics of either fuel alone. Consequently, understanding the co-combustion dynamics is essential, motivating a growing body of research in this area. Qin et al. [4] investigated the co-combustion characteristics of Indonesian coal, Shaanxi coal, Datong coal, and eucalyptus wood using thermogravimetric analysis (TGA). The results showed that compared with pure coal combustion, co-firing with eucalyptus wood could improve combustion efficiency and reduce activation energy. During the co-firing process, there were interactions between the three types of coal and eucalyptus wood; among them, Shaanxi coal and eucalyptus wood exhibited a relatively obvious promoting effect, while the other two types of coal and eucalyptus wood showed more antagonistic effects. Luo and Zhou [5] conducted co-combustion studies using three types of coal and four types of biomass, and concluded that ash content played a dominant role in the interaction between biomass and coal. Coal with low ash content was more likely to react with biomass during combustion, showing a significant synergistic effect, while there was almost no synergistic effect between coal with high ash content and biomass. Si et al. [6] investigated the co-combustion process of three typical types of biomass and bituminous coal using TGA, and calculated their kinetic parameters. The results showed that the combustion mechanisms of the three mixed fuels all conformed to the diffusion mechanism model; the activation energy of co-combustion decreased due to the influence of the high volatile content of biomass, which proved that the addition of biomass could improve the combustion performance of bituminous coal. From the above studies, it can be seen that due to the wide variety of biomass types and large differences in their compositions, the effects of different biomass on the co-firing process and the reaction mechanism of the combustion process still remain controversial. Furthermore, previous studies mainly studied the interaction between coal and biomass by comparing the difference between actual and theoretical thermal weight loss, which overlooks the potential varying effects of the interaction that may occur in different combustion stages.

Controlling pollutant emissions is also crucial in energy utilization. The emission levels of pollutants not only affect the fuel utilization efficiency but also relate to the cost of flue gas purification facilities. Numerous studies have shown that the co-firing of coal and biomass can reduce pollutant emissions. Ji et al. [7] co-fired peanut shells with coal and found that when the blending ratio of peanut shells reached 40 %, not only the emissions of SO_2 , NO_x , and particulate matter were significantly reduced, but also the CO_2 emissions could be decreased. Fan et al. [8] studied the pollutant emission

characteristics during the co-firing of eucalyptus wood and coal using a horizontal tubular furnace. The results showed that the contents of NO and SO₂ in the flue gas decreased with the increase of blending ratio and temperature, and the decrease of NO and SO₂ was most significant when the blending ratio of eucalyptus wood was 5 %–15 %. Zhou et al. [9] investigated the co-combustion process of medium-low ash bituminous coal with corn stover and sawdust in a vacuum tubular furnace. It was found that in addition to conventional gaseous pollutants, the addition of corn stover and sawdust could also reduce the emissions of PAHs and trace elements such as As and Cd. However, the biomass selected in existing studies usually has low nitrogen (N) content, and whether biomass with high N content can reduce NO_x emissions remains to be explored. Moreover, most studies on pollutant emission reduction effects are based on equipment such as tubular furnaces, and there is a lack of research under high-temperature and dynamic environments that simulate industrial pulverized coal furnaces.

Based on these, this study selected two types of biomass—rice husks (RH) with low N content and *Populus tomentosa* sawdust (SD) with high N content—for co-firing with coal, and conducted a comprehensive study on the effects of their coupled combustion. This study covers aspects such as coupled combustion characteristics and pollutant emission characteristics, and analyzes the interaction between coal and biomass during different combustion stages, as well as the effect of biomass with high N content on NO_x emission reduction.

2 Materials and methods

2.1 Raw materials and sample preparation

Table 1 Proximate and ultimate analyses of coal, RH, and SD

Fuel	Proximate analysis/%				Ultimate analysis/%				
	M _{ad}	A _{ad}	V _{ad}	FC _{ad}	C _{ad}	H _{ad}	O _{ad}	N _{ad}	S _{ad}
Coal	5.96	25.5	26.6	42.0	57.1	2.93	6.54	1.43	0.63
RH	9.39	12.6	64.1	13.9	38.0	4.81	34.2	0.94	0.00
SD	8.76	1.94	76.0	13.3	43.5	5.37	36.1	4.33	0.00

Table 2 Ash Composition analysis of coal, RH, and SD (wt.%)

Fuel	Na ₂ O	MgO	Al ₂ O ₃	SiO ₂	P ₂ O ₅	SO ₃	K ₂ O	CaO	MnO	Fe ₂ O ₃
Coal	0.22	0.45	50.8	36.6	0.26	2.72	0.57	4.08	0.02	2.48
RH	0.41	0.99	0.77	88.3	2.98	0.84	3.57	1.04	0.36	0.51
SD	8.72	30.8	2.53	6.68	6.76	9.14	3.65	29.7	0.10	1.24

The base fuel employed in this study was Shenhua bituminous coal. Biomass samples, namely rice husk (RH) and *Populus tomentosa* sawdust (SD), were collected from the Lianyungang region. The raw materials were dried in a blast drying oven at 105 °C for 2 hours, then crushed and sieved. Powder with a particle size between 80 and 100 mesh was collected, and mixed samples were prepared with the mass proportion of biomass set at 5 %, 15 %, and 25 %, respectively. Table 1 summarizes the proximate and ultimate analyses of the raw coal and biomass feedstocks, illustrating distinct differences in volatile matter, ash content, and elemental composition. The ash compositions of coal and biomass were analyzed using an X-ray fluorescence spectrometer (PANalytical Zetium, Netherlands), and the results

are shown in Table 2.

2.2 Experimental apparatus and methods

Combustion behavior was assessed using a thermogravimetric analyzer (Rigaku TGA-DTA8122, Japan). Approximately 5 mg of sample was uniformly placed in an alumina crucible and heated from ambient temperature to 1000 °C at 10 °C/min under an air flow of 50 mL/min.

Several key indices were employed to quantify the combustion characteristics of the fuels:

- Ignition temperature (T_i): Representing the fuel's ignitability, a higher T_i denotes greater difficulty in ignition. In this work, T_i was identified using the TG-DTG tangent intersection method [10].
- Burnout temperature (T_b): This parameter, defined as the point where 98 % of the total weight loss has occurred, reflects the completeness of combustion; an elevated T_b suggests slower burnout kinetics.
- Comprehensive combustion index (S): To holistically assess combustion performance, the index S was calculated. An increase in the S value corresponds to enhanced overall combustibility. Its calculation formula is as follows:

$$S = \frac{(dw/dt)_{\max} \cdot (dw/dt)_{\text{mean}}}{T_i^2 \cdot T_b} \quad (1)$$

In the formula, $(dw/dt)_{\max}$ and $(dw/dt)_{\text{mean}}$ respectively represent the maximum mass loss rate and the average mass loss rate at the burnout temperature, with the unit of %/min.

To further investigate the interaction between biomass and coal during the co-firing process, the TG-DTG curves of mixed samples were compared with the theoretical curves obtained by mass-weighted average. The calculation formula is as follows:

$$TG_{\text{cal}} = (1-x)TG_{\text{c-exp}} + xTG_{\text{bio-exp}} \quad (2)$$

In the formula, TG_{cal} is the theoretical TG value of the mixed sample assuming no synergistic effect; $TG_{\text{c-exp}}$ and $TG_{\text{bio-exp}}$ are the experimental TG values of coal and biomass during individual combustion, respectively; and x is the blending ratio of biomass.

The deviation ΔTG caused by the interaction is calculated using the following formula:

$$\Delta TG = TG_{\text{cal}} - TG_{\text{exp}} \quad (3)$$

$\Delta TG < 0$ indicates that the interaction manifests as a synergistic effect, while $\Delta TG > 0$ indicates that the interaction manifests as an antagonistic effect.

The activation energy (E) of the combustion process was derived utilizing the Coats-Redfern integral method, expressed by Equation (4):

$$\ln \frac{G(\alpha)}{T^2} = \ln \left[\frac{AR}{\beta E} \left(1 - \frac{2RT}{E} \right) \right] - \frac{E}{RT} \quad (4)$$

In the formula, α is the mass loss rate; T is the thermodynamic temperature, with the unit of K; A is the pre-exponential factor, with the unit of min^{-1} ; R is the gas constant; β is the heating rate; and $G(\alpha)$ is the reaction mechanism model.

This study selected 7 reaction models [6] for fitting, and the one with the highest correlation

coefficient was chosen to describe the combustion process. The expressions of the 7 reaction models are shown in Table 3:

Table 3 Reaction models

Model	G(α)
First order - O1	$-\ln(1-\alpha)$
Contracting cylinder - P1	$1-(1-\alpha)^{1/2}$
Contracting sphere - P2	$1-(1-\alpha)^{1/3}$
1D diffusion - D1	α^2
2D diffusion - D2	$(1-\alpha)\ln(1-\alpha)+\alpha$
Jander,3D - D3	$[1-(1-\alpha)^{1/3}]^2$
Ginstling-Brounshtein,3D - D4	$1-2\alpha/3-(1-\alpha)^{2/3}$

The pollutant emission characteristics experiment of mixed fuels was conducted in a DTF (Yixing Shangneng Furnace Industry Co., Ltd., Model FD1300100). The corundum tube of this system has a total length of 1900 mm, and the total length of the heating section is approximately 1500 mm. The operating temperature of the DTF was set at 1100 °C, and the excess air coefficient was 1.4.

Before the experiment, the temperature-rising program and air compressor were started to purge residual gases in the furnace. When the furnace temperature rose to the target temperature, the flue gas analyzer (MRU, Germany, Model MGA5) was turned on. Then, 25 g of uniformly mixed materials was added to the screw feeder, and the materials were carried into the drop tube furnace by air for combustion, with a combustion duration of approximately 30 min. Due to the instability of feeding and air intake during the experiment, there were still slight fluctuations in gas concentration even after it stabilized. Therefore, the integral average value of the data recorded by the flue gas analyzer was taken as the experimental result. For the convenience of comparison, all gas concentrations were converted to the concentrations under 6 % oxygen content. After the reaction, the feeder and air valves were closed. After cooling, the ash hopper valve was opened to sample the bottom slag. The flue gas generated in the experiment was passed through the cyclone separator, gas line filter, and absorption bottle in sequence to remove fly ash, fine particles, and harmful gases before being discharged outside the window.

To study the synergistic effect of coal and biomass in pollutant emission reduction during the co-firing process, the theoretical values of pollutant emissions are obtained by mass proportion-weighted average, and the calculation formula is as follows:

$$G_{cal} = (1-x)G_{c-exp} + xG_{bio-exp} \quad (5)$$

In the formula, G_{cal} represents the theoretical value of pollutant concentration, with the unit of mg/Nm³; G_{c-exp} and $G_{bio-exp}$ respectively denote the pollutant emission concentrations of coal and biomass during individual combustion, with the unit of mg/Nm³.

3 Results

3.1 Analysis of combustion characteristics

3.1.1 Analysis of thermogravimetric process

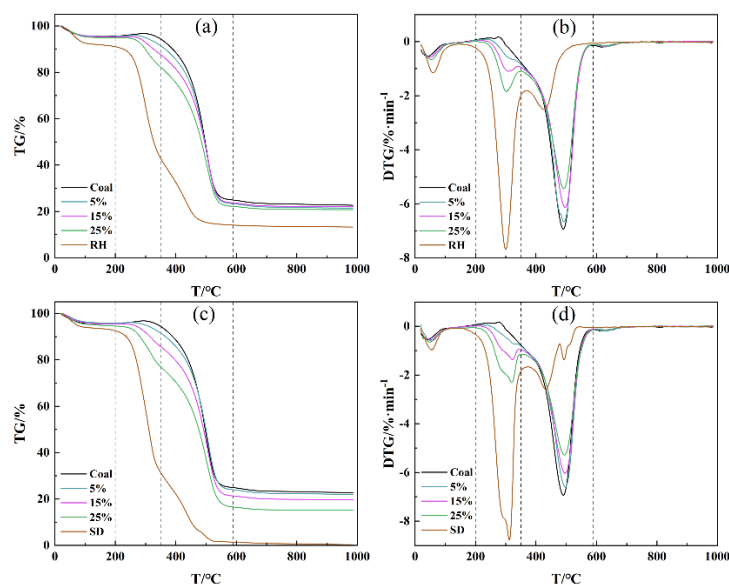


Fig. 1 TG curves for co-firing RH (a), DTG curves for co-firing RH (b), TG curves for co-firing SD (c), DTG curves for co-firing SD (d)

As shown in Fig. 1, when co-fired at a low blending ratio, the co-combustion characteristics are more similar to those of pure coal combustion, with only two relatively obvious weight loss peaks observed on the DTG curve. With the increase of blending ratio, the TG curve shows a tendency to shift to the low-temperature region. When the blending ratio is $\geq 15\%$, the DTG curve of the mixed fuel begins to exhibit the double-peak characteristic similar to that of biomass combustion alone during the rapid weight loss stage. Therefore, this stage can be divided into the volatile release and combustion stage (200–350 °C) and the fixed carbon combustion stage (350–590 °C). The difference is that due to the high proportion of coal, the combustion is still dominated by fixed carbon, and the maximum weight loss peak appears around 500 °C, with its peak value decreasing as the blending ratio increases. Although the peak value of the weight loss peak formed by volatile release increases with the increase of blending ratio, its intensity remains weak under the experimental conditions selected, and the highest value is only 2.31 %/min when the blending ratio of SD is 25 %.

Table 4 Combustion characteristic parameters of mixed fuels

Blending ratios	0 %	5 %		15 %		25 %		100 %	
		RH	SD	RH	SD	RH	SD	RH	SD
$T_i/^\circ\text{C}$	437	431	434	425	421	407	397	261	256
$T_b/^\circ\text{C}$	628	608	621	588	584	574	571	512	516
$(dw/dt)_{\max}/\% \cdot \text{min}^{-1}$	6.94	6.66	6.60	6.14	6.04	5.43	5.28	7.68	8.77
$(dw/dt)_{\text{mean}}/\% \cdot \text{min}^{-1}$	1.09	1.19	1.14	1.22	1.28	1.27	1.37	1.53	1.75
$S \cdot 10^7/\%^2 \cdot \text{min}^{-2} \cdot ^\circ\text{C}^{-3}$	0.63	0.70	0.64	0.71	0.75	0.73	0.80	3.37	4.52

The combustion characteristic parameters, compiled in Table 4, reveal that blending with RH or SD consistently lowered both the T_i and T_b relative to pure coal, and the improvement was more pronounced at higher blending ratios. This is mainly because cellulose and hemicellulose in biomass are more likely to pyrolyze at low temperatures, releasing a large amount of volatile substances that burn

rapidly [11], thereby promoting the early ignition of pulverized coal. In addition, the lower ash content and fixed carbon content in biomass also make the mixed fuel easier to burnout. From the perspective of the comprehensive combustion index S , co-firing with biomass is always beneficial to improving combustion performance. Compared with RH, when the blending ratio is $\geq 15\%$, co-firing with SD leads to a greater improvement in combustion performance. This is not only due to the higher volatile content in SD, but also related to the catalytic effect of the higher alkali metal and alkaline earth metal contents in SD on coal combustion [12].

3.1.2 Analysis of synergistic effect

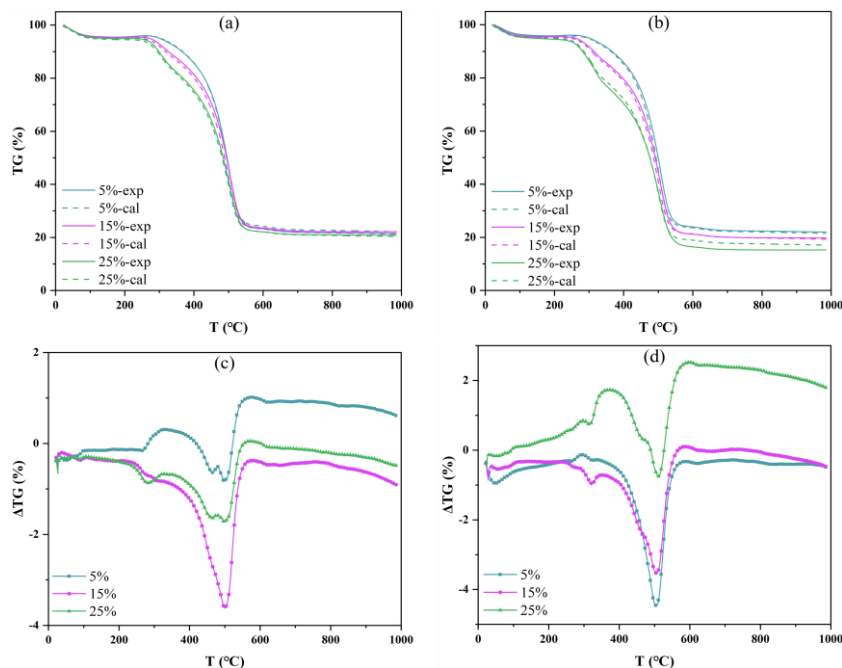


Fig. 2 Experimental (exp) and theoretical (cal) TG curves for co-firing RH (a) and WC (b) at different ratios, and deviations caused by the interaction between coal and RH (c)/SD (d)

While the sign of ΔTG is frequently employed to classify overall synergistic or antagonistic interactions [4], interpreting stage-specific effects requires caution because ΔTG values accumulate across successive reaction stages. For example, in stage n , the interaction significantly promotes combustion, making ΔTG much less than 0; even if the interaction inhibits combustion in stage $n+1$, ΔTG may still be less than 0. So, it is inappropriate for some researchers [13, 14] to use this method to judge the interaction in each combustion stage. Therefore, this study uses the positive or negative value of the slope of the ΔTG curve to determine whether the interaction in each combustion stage is synergistic or antagonistic.

Discrepancies between the experimental and calculated TG trajectories (Fig. 2a, b) provide direct evidence of interactions between coal and biomass during co-combustion. From the final effect, only when co-fired with 5% RH and 25% SD, the actual total weight loss is greater than the theoretical value, and the co-firing exhibits a synergistic effect; under other conditions, it exhibits a slight antagonistic effect. The slope of ΔTG further reflects the comparison between the actual weight loss rate and the theoretical value. When the ΔTG curve rises, it means that the actual weight loss rate is greater than the theoretical weight loss rate. It can be found that in the main combustion temperature range of

400–570 °C, the ΔTG is always bounded by approximately 500 °C, first decreasing and then increasing. This phenomenon can also be observed in the study by Lei et al. [15], with slight differences in the threshold temperature due to the different raw materials used. This indicates that even though ΔTG is always less than 0, the interaction between coal and RH/SD shifts from inhibitory to promotional, and the promoting effect is greater than or approximately equal to the inhibiting effect. It can be seen that whether the interaction eventually manifests as a synergistic or antagonistic effect mainly depends on its influence on the weight loss rate during the dehydration and devolatilization stages before 400 °C.

3.1.3 Study on reaction kinetics

Table 5 Calculation of Reaction Kinetics Parameters

Samples	Stage 2 (200–350 °C)			Stage 3 (350–590 °C)		
	E/kJ·mol ⁻¹	Model	R ²	E/kJ·mol ⁻¹	Model	R ²
Coal	–	–	–	116	D3	0.98
With 5 % RH	–	–	–	95.9	D4	0.97
With 15 % RH	27.2	D3	0.71	68.9	D1	0.97
With 25 % RH	39.0	D1	0.83	60.7	D2	0.97
RH	65.0	D1	0.95	14.5	D3	0.72
With 5 % SD	–	–	–	91.8	D2	0.98
With 15 % SD	34.2	D1	0.84	63.6	D1	0.97
With 25 % SD	46.4	D1	0.92	45.2	D1	0.96
SD	79.3	D1	0.97	24.8	D3	0.94

As pointed out earlier, when the biomass blending ratio is $\geq 15\%$, there are two peaks in the rapid weight loss region. Based on this, the rapid weight loss region is divided into the volatile removal and combustion stage (Stage 2) and the fixed carbon combustion stage (Stage 3), and these two stages are fitted separately. When the blending ratio is 5 % or lower, only one peak exists, so only Stage 3 was fitted. The fitting results are shown in Table 5: the combustion processes of coal, RH, SD and their mixtures are mainly controlled by the diffusion mechanism. In Stage 2, the correlation coefficient of D1 is almost always the highest. As the blending ratio increases, both the activation energy required for combustion and the model fitting accuracy increase. Due to the lower volatile content of RH, the activation energy required for combustion when co-firing with RH is always lower than that when co-firing with SD under the same blending ratio at this stage. In Stage 3, as the blending ratio increases, the activation energy required for combustion gradually decreases, indicating that co-firing with biomass can effectively promote the combustion of fixed carbon. The porosity formed after more volatile release enhances the contact between coke and oxygen [16], which leads to a gradual decrease in the activation energy required for combustion in the stage 3 as the blending ratio increases. The minimum activation energy principle can help determine the optimal biomass blending ratio; however, the actual combustion process involves multiple aspects such as gaseous pollutants, heavy metals, and ash, requiring comprehensive consideration.

3.2 Pollutant emissions and ash formation characteristics

3.2.1 Influence of biomass blending on NO_x and SO_2 emissions

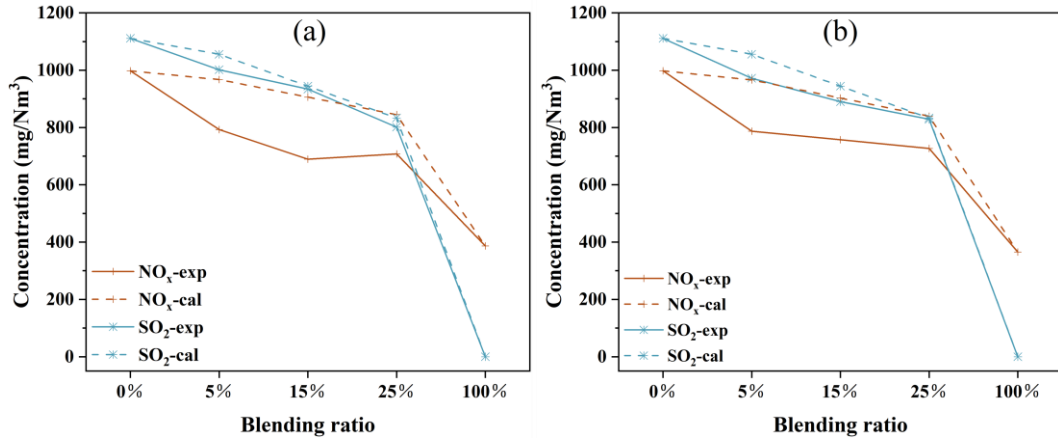


Fig. 3 Pollutant concentrations during co-firing RH (a) and WC (b) at different blending ratios

Biomass blending proportion markedly influenced the co-combustion performance. As illustrated in Fig. 3, both NO_x and SO_2 emissions decreased progressively with higher biomass shares. Compared with pure coal combustion, when co-fired with different ratios of RH, the reduction rates of NO_x were 20.5 %, 30.9 %, and 29.1 % respectively; when co-fired with different ratios of SD, the reduction rates of NO_x were 21.1 %, 24.1 %, and 27.2 % respectively.

As the biomass blending ratio increases, although the overall volatile fraction continues to rise, the reduction rate of NO_x gradually decreases. Even when the blending ratio of rice husks increases from 15 % to 25 %, the concentration of NO_x even increases slightly. This may be related to the higher moisture content in rice husks leading to ignition delay [17]. It can be seen that an increase in the biomass blending ratio does not necessarily bring better NO_x emission reduction effects, which is consistent with the research of Savolainen [18].

In terms of SO_2 emission reduction, the increase in biomass blending ratio shows a significant positive correlation with the decrease in SO_2 concentration. Compared with pure coal combustion, when co-fired with different ratios of RH, the reduction rates of SO_2 were 9.87 %, 15.9 %, and 27.9 % respectively; when co-fired with different ratios of SD, the reduction rates of SO_2 were 12.5 %, 19.9 %, and 25.4 % respectively. This mainly because the RH and SD used in the experiment do not contain sulfur; all SO_2 in the flue gas comes from coal. As the proportion of coal decreases, the SO_2 concentration decreases accordingly.

Through the comparison between theoretical values and experimental values, it can be seen that coal and biomass exhibit a strong synergistic effect in terms of NO_x emission reduction, which is mainly attributed to the high volatile content in biomass. Previous research has noted that biomass contains abundant alkali metals and alkaline earth metals, which function as desulfurization agents during combustion [19]. Thus, in terms of SO_2 emission reduction, there is also a synergistic effect between coal and biomass. However, this synergistic effect is not obvious. The difference between the theoretical and experimental values of SO_2 concentration is small, with the maximum difference being only 7.95 % (when co-firing with 5 % SD). This indicates that sulfur content is the main factor affecting SO_2 emission

concentration.

Compared with SO₂, the formation pathways of NO_x are more complex. To further clarify the NO_x reduction mechanism of biomass co-firing, a reaction model was constructed in this paper, as shown in Fig. 4. Most of the N in biomass exists in the form of amino-N, which is released with volatile emission in the early stage of combustion, producing a large amount of N-containing precursors such as NH₃ (predominantly) and HCN (a small amount) [20-22]. On the one hand, these N-containing precursors will be converted to NO_x under oxygen-sufficient conditions; on the other hand, they also have a reducing effect on NO_x [23]. During coal-biomass co-firing, biomass volatiles burn intensely, rapidly consuming oxygen and forming a local oxygen-lean atmosphere. This condition suppresses the transformation of nitrogen-containing precursors into NO_x while facilitating the reduction of existing NO_x, ultimately lowering emissions. This also explains why the N content of SD is much higher than that of RH, but its actual NO_x emission reduction effect is only slightly lower than that of RH. Higher fuel nitrogen content in SD increases the concentration of NH_i radicals in volatiles, which leads to the formation of thermal De-NO_x [24] at an appropriate temperature, resulting in an increased degree of NO reduction. Similar observations were reported by Giuntoli et al. [25].

In addition, gases such as CO and H₂ contained in volatiles can reduce the generated NO through homogeneous reactions, and the relevant reaction equations are as follows [26]:

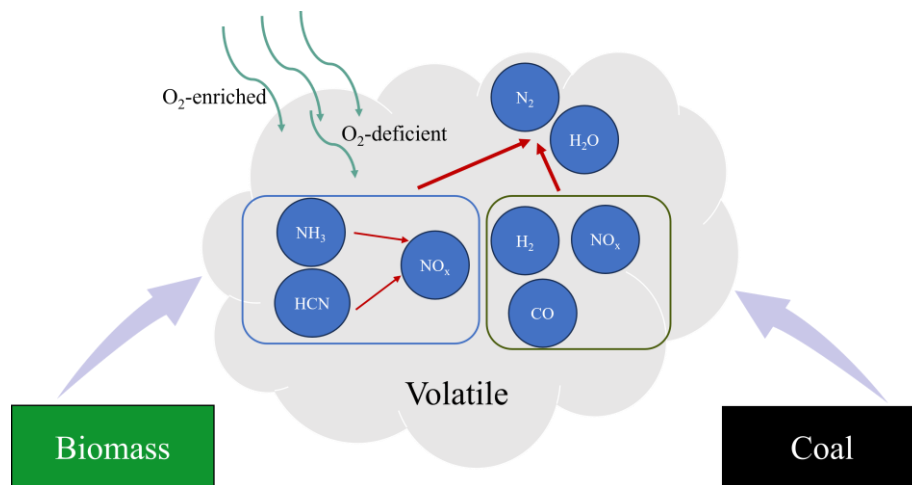
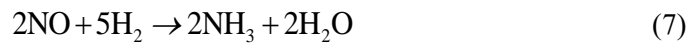


Fig. 4 NO_x emission reduction mechanism

5 Conclusion

The main findings of this study are summarized as follows:

(1) Kinetic analysis confirmed that the combustion of all fuels and their blends was governed primarily by a diffusion mechanism, with biomass addition consistently enhancing combustibility by lowering ignition and burnout temperatures.

(2) The positive or negative value of the slope of the ΔTG curve can be used to judge the interaction between coal and biomass during the coupled combustion process. During the coupled combustion process, synergistic effects and antagonistic effects alternate.

(3) In terms of emissions, SO₂ reduction was directly attributable to the low sulfur content of the biomass, while effective NO_x reduction—even with high-nitrogen SD—was facilitated by a volatile-induced reducing atmosphere that suppressed the fuel-N to NO_x conversion pathway.

Acknowledgement

This work was supported by the National Key Research and Development Program of China (2024YFB4106103).

References

- [1] Wang, X., *et al.*, Analysis of the effect of ammonia on 300 MW pulverized coal boiler fuel gas characteristics. *Electric Power Technology and Environmental Protection*, 41 (2025), pp. 294-302.
- [2] Wen, X., *et al.*, Preparation of plant-based activated carbon and its application in the field of power generation. *Electric Power Technology and Environmental Protection*, 41 (2025), pp. 393-404.
- [3] Zhu, F., *et al.*, Opportunities and challenges of coal power industry in the achievement of carbon neutrality goal. *Electric Power Technology and Environmental Protection*, 38 (2022), pp. 79-86.
- [4] Qin, S., *et al.*, Co-combustion characteristics, interaction and kinetic analysis of multiple coal and eucalyptus. *Industrial Crops and Products*, 222 (2024), pp. 119980.
- [5] Luo, R. and Q. Zhou, Combustion kinetic behavior of different ash contents coals co-firing with biomass and the interaction analysis. *Journal of Thermal Analysis and Calorimetry*, 128 (2017), 1, pp. 567-580.
- [6] Si, F., *et al.*, Thermodynamics and synergistic effects on the co-combustion of coal and biomass blends. *Journal of Thermal Analysis and Calorimetry*, 149 (2024), 14, pp. 7749-7761.
- [7] Ji, L., *et al.*, Coal Blending with Peanut Shells: Thermal Behavior, Kinetics, Carbon Reduction and Pollution Reduction Analyses. *Water, Air, & Soil Pollution*, 235 (2024), 10, pp. 634.
- [8] Fan, Z., *et al.*, Experimental study on co-combustion of eucalyptus and coal. *Journal of Huazhong University of Science and Technology (Natural Science Edition)*, 53 (2025), pp. 92-99.
- [9] Zhou, C., *et al.*, Co-combustion of bituminous coal and biomass fuel blends: Thermochemical characterization, potential utilization and environmental advantage. *Bioresource Technology*, 218 (2016), pp. 418-427.
- [10] Ma, B.-G., *et al.*, Investigation on catalyzed combustion of high ash coal by thermogravimetric analysis. *Thermochimica Acta*, 445 (2006), 1, pp. 19-22.
- [11] Wu, Z., *et al.*, Synergistic effect on thermal behavior during co-pyrolysis of lignocellulosic biomass model components blend with bituminous coal. *Bioresource Technology*, 169 (2014), pp. 220-228.
- [12] Ruan, R., *et al.*, The effect of alkali and alkaline earth metals (AAEMs) on combustion and PM formation during oxy-fuel combustion of coal rich in AAEMs. *Energy*, 293 (2024), pp. 130695.
- [13] Guo, Z., *et al.*, Co-pyrolysis and co-combustion characteristics of low-rank coal and waste biomass: Insights into interactions, kinetics and synergistic effects. *Journal of the Energy Institute*, 118 (2025), pp. 101918.

- [14] Liu, N., et al., Co-pyrolysis Behavior of Coal and Biomass: Synergistic Effect and Kinetic Analysis. *ACS Omega*, 9 (2024), 29, pp. 31803-31813.
- [15] Lei, M., et al., Analysis and prediction of combustion characteristics of co-combustion of coal and biomass (straw, sludge and herb residue). *Journal of Thermal Analysis and Calorimetry*, 150 (2025), 3, pp. 1741-1755.
- [16] Rago, Y.P., et al., Co-combustion of torrefied biomass-plastic waste blends with coal through TGA: Influence of synergistic behaviour. *Energy*, 239 (2022), pp. 121859.
- [17] Munir, S., W. Nimmo, and B.M. Gibbs, The effect of air staged, co-combustion of pulverised coal and biomass blends on NO_x emissions and combustion efficiency. *Fuel*, 90 (2011), 1, pp. 126-135.
- [18] Savolainen, K., Co-firing of biomass in coal-fired utility boilers. *Applied Energy*, 74 (2003), 3, pp. 369-381.
- [19] Rokni, E., H. Hsein Chi, and Y.A. Levendis, In-Furnace Sulfur Capture by Cofiring Coal With Alkali-Based Sorbents. *Journal of Energy Resources Technology*, 139 (2017), 4.
- [20] Chen, H., et al., NO_x precursors from biomass pyrolysis: Distribution of amino acids in biomass and Tar-N during devolatilization using model compounds. *Fuel*, 187 (2017), pp. 367-375.
- [21] Wang, Y., et al., N migration and transformation during the co-combustion of sewage sludge and coal slime. *Waste Management*, 145 (2022), pp. 83-91.
- [22] Abelha, P., I. Gulyurtlu, and I. Cabrita, Release Of Nitrogen Precursors From Coal And Biomass Residues in a Bubbling Fluidized Bed. *Energy & Fuels*, 22 (2008), 1, pp. 363-371.
- [23] Wang, Y., et al., Experimental investigation of the characteristics of NO_x emissions with multiple deep air-staged combustion of lean coal. *Fuel*, 280 (2020), pp. 118416.
- [24] Kasuya, F., et al., The thermal DeNO_x process: Influence of partial pressures and temperature. *Chemical Engineering Science*, 50 (1995), 9, pp. 1455-1466.
- [25] Giuntoli, J., et al., Combustion Characteristics of Biomass Residues and Biowastes: Fate of Fuel Nitrogen. *Energy & Fuels*, 24 (2010), 10, pp. 5309-5319.
- [26] Nimmo, W., S.S. Daood, and B.M. Gibbs, The effect of O₂ enrichment on NO_x formation in biomass co-fired pulverised coal combustion. *Fuel*, 89 (2010), 10, pp. 2945-2952.

Submitted: 26.12.2025

Revised: 24.02.2026

Accepted: 03.03.2026